NANO LETTERS

2006
Vol. 6, No. 7
1529−1534

Effect of Aggregation Kinetics on the Thermal Conductivity of Nanoscale Colloidal Solutions (Nanofluid)

Ravi Prasher*

Intel Corporation, CH5-157, 5000 West Chandler Boulevard, Chandler, Arizona 85226-3699

Patrick E. Phelan and Prajesh Bhattacharya

Arizona State University, Department of Mechanical & Aerospace Engineering, Tempe, Arizona 85287-6106

Received May 2, 2006; Revised Manuscript Received June 4, 2006

ABSTRACT

The thermal conductivity, *k*, of nanoscale colloidal suspensions (also known as nanofluid), consisting of nanoparticles suspended in a base liquid, is much higher than the thermal conductivity of the base liquid at very small volume fractions of the nanoparticles. However, experimental results from various groups all across the world have shown various anomalies such as a peak in the enhancement of *k* with respect to nanoparticle size, an increase as well as a decrease in the ratio of *k* of these colloidal solutions with the *k* of the base fluid with increasing temperature, and a dependence of *k* on pH and time. In this paper, the aggregation kinetics of nanoscale colloidal solutions are combined with the physics of thermal transport to capture the effects of aggregation on *k*. Results show that the observed anomalies reported in experimental work can be well described by taking aggregation kinetics into account. Finally, we show that colloidal chemistry plays a significant role in deciding the *k* of colloidal nanosuspensions.

Experimental data[1−7] have shown that nanoscale colloidal solutions, also known as nanofluids (NFs), have much higher thermal conductivity (k) than can be predicted using classical conduction models, such as the Maxwell−Garnett (MG) model[8−10] for well-dispersed particulate composites. Currently, there are two lines of thinking for explaining the enhancement in k: (1) k is enhanced by microconvection caused by the Brownian motion (BM) of the nanoparticles,[8−12] and (2) k is enhanced due to the aggregation of the nanoparticles leading to local percolation behavior.[13−15] Both these explanations for k are independent of one other, whereas the colloidal literature clearly indicates that BM and aggregation are related.[16−17] Depending on the chemistry of the system, rapid aggregation of particles can take place. Figure 1 schematically shows aggregation. The probability of aggregation increases with decreasing particle size, at constant volume fraction, because the average interparticle distance decreases, making the attractive van der Waals force more important.[16−17] Aggregation will decrease the BM due to the increase in the mass of the aggregates, whereas it can increase k due to percolation effects in the aggregates, as highly conducting particles touch each other in the aggregate. Existing BM microconvection models for k, however, do not consider aggregation,[8−12] and existing aggregation models for k do not consider aggregation kinetics.[13−15]

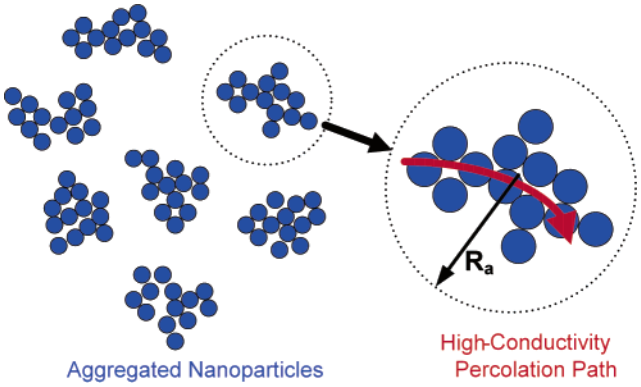

Figure 1. Schematic of well-dispersed aggregates. The aggregates are characterized by their radius of gyration (R_a). Aggregates have a higher mass than individual particles.

Bordi et al.[18] showed experimentally that the electrical conductivity of colloids depends on the aggregation kinetics of the system. Aggregation is a time-dependent phenomenon.[15−17] Therefore, initially the particles will be well

* To whom correspondence should be addressed. E-mail: ravi.s.prasher@intel.com. Also at Arizona State University, Department of Mechanical & Aerospace Engineering.

10.1021/nl060992s CCC: $33.50
Published on Web 06/15/2006

dispersed at $t = 0$ (t = time) and then will start to agglomerate to form multiple aggregates as shown in Figure 1. Aggregates are characterized by their radius of gyration (R_a) as shown in Figure 1. These individual aggregates will have higher conductivity than the liquid; they can be considered as the new "particles" with an effective radius of R_a and they will enhance the k of the NF. However, this enhancement will decrease as the aggregates continue to agglomerate to make much bigger aggregates. As $t \rightarrow \infty$, all the nanoparticles will agglomerate to form one large aggregate, at which time the nanoparticles will not enhance k further. Therefore, the enhancement in k due to aggregation will be maximum for well-dispersed aggregates, somewhere between the two extremes at $t = 0$ (no aggregation) and $t \rightarrow \infty$ (complete aggregation). The NF aggregation models in the literature have so far ignored this aspect. If ϕ_p is the volume fraction of the primary particles, ϕ_{int} the volume fraction of the particles in the aggregates, and ϕ_a the volume fraction of the aggregates in the entire fluid, then $\phi_p = \phi_{int}\phi_a$. Note that the aggregate is described by a sphere of size R_a—larger than the radius of a single nanoparticle—as shown in Figure 1. The relation $\phi_p = \phi_{int}\phi_a$ shows that, for a well-dispersed system, $\phi_{int} = 1$, as there is only one particle in each aggregate and $\phi_a = \phi_p$, whereas for a completely aggregated system $\phi_a = 1$ and $\phi_{int} = \phi_p$. The maximum k due to conduction will occur between these two limits.

On the experimental front, various anomalies have been reported. These anomalies include: (1) A maximum in the enhancement of k with respect to (wrt) the diameter of nanoparticles.[1] (2) The effect of aging.[4] (3) An increase in k by adding acid[4] and a decrease in k with increasing pH.[1] (4) An increase in k wrt sonication time.[6] (5) An effect of surface treatment on k.[7] (6) An increase in the k enhancement for carbon nanotube (CNT) based NFs[19] wrt temperature. The increase in the k enhancement wrt temperature has been associated with an increase in the BM of the nanoparticles,[8−12] however for CNTs it seems unlikely that there will be any significant BM. Various groups have also shown through imaging that nanoparticles are well dispersed as well as severely agglomerated, depending on particle type and surface treatment.[1−7,13−15]

Modeling the Effects of Aggregation and Brownian-induced Convection. In this paper, we develop a unified model which combines the microconvective effects due to BM with the change in conduction due to aggregation. For simplicity, we have ignored the effects of thermal boundary resistance between the particles and the fluid. Quantitative comparison is made with the experimental data collected by us on nanofluids made from different sizes of nanoparticles. For some of the other anomalies, however, qualitative comparisons are presented because most of the relevant parameters have not been reported in the literature. This paper resolves some of the conflicts that exist in the experimental literature and also provides guidance to experimentalists for future studies. Particles are assumed to be spherical and of uniform size. The subscripts a and p denote variables related to the aggregates and primary nanoparticles, respectively.

The Brownian velocity is given by

$$v = \sqrt{3k_B T/m} \tag{1}$$

where k_B is the Boltzmann constant, T the temperature, and m the mass, where $m = m_p = 4/3\pi r_p^3 \rho_p$ for a well-dispersed system, where r_p is the radius of the primary particles and ρ_p is the density of the nanoparticles, and $m = m_a$ for an aggregated system. Aggregates are characterized by their radius of gyration, R_a, as mentioned earlier. Through the use of the Smoluchowski model, the average R_a is given by[20]

$$R_a/r_p = (1 + t/t_p)^{1/d_f} \tag{2}$$

where t_p is the aggregation time constant and d_f the fractal dimension of the aggregates. Previous studies have indicated that d_f ranges from 1.75 to 2.5.[16,17,21] For a strong repulsive barrier, $d_f \approx 2.5$, which signifies reaction-limited aggregation, whereas for a weak repulsive barrier $d_f = 1.8$ which signifies diffusion-limited cluster−cluster aggregation (DLCCA).[16−17] Waite et al.[21] conducted a thorough study of aggregation of nanosized alumina suspensions and found that d_f ranged from 1.8 to 2.3. Wang et al.[13] have shown that in NF aggregation is DLCCA, as the fractal dimensions are close to 1.8 which signifies DLCCA. Therefore, $d_f = 1.8$ is assumed for these calculations, however the model is valid for any d_f. The number of particles in a single aggregate (N_{int}) is given by[20]

$$N_{int} = (R_a/r_p)^{d_f} = (1 + t/t_p) \tag{3}$$

Therefore, the total mass of the particles in a single aggregate is given by

$$m_a = m_p(1 + t/t_p) \tag{4}$$

The aggregation time constant is given by[20]

$$t_p = (\pi\mu r_p^3 W)/(k_B T \phi_p) \tag{5}$$

where μ is the viscosity of the liquid and W the stability ratio. This equation shows that t_p decreases rapidly for decreasing particle radius r_p, which means rapid aggregation can take place for smaller particles. Note that only for $t_p \rightarrow \infty$ is the system stable and well dispersed. The stability ratio $W = 1$ in the absence of a repulsive force and hydrodynamic interactions between the nanoparticles, and in the presence of a repulsive force, $W > 1$. Derjaguin−Landau−Verwey−Overbeck (DLVO) theory is used to model the repulsive (V_R) and attractive (V_A) potential energies between the nanoparticles[16,17] to calculate W. V_A between two spheres is modeled using[16]

$$V_A = -A/6[2r_p^2/h(h + 4r_p) + 2r_p^2/(h + 2r_p)^2 + \ln(h(h + 4r_p)/(h + 2r_p)^2)] \tag{6}$$

where A is the Hamaker constant and h the interparticle distance. V_R is modeled using[16−17]

$$V_R = 2\pi\epsilon_r\epsilon_0 r_p \Psi^2 \exp(-\Lambda h) \quad (7)$$

where ϵ_r is the relative dielectric constant of the liquid, ϵ_0 the dielectric constant of free space, Ψ the ζ potential, and Λ the Debye parameter (inverse of the Debye length). Note that eq 7 is valid for $\Lambda r_p < 5$, which means that it is valid for a larger Debye length or smaller r_p. This equation will be valid for nanofluids in the absence of electrolytes such as salt because Λ is small for water[22] and because r_p is very small for nanoparticles. However, various expressions for V_R for different and general values of Λr_p are readily available in the colloidal literature. For water,[22] Λ can be written as

$$\Lambda = 5.023 \times 10^{11}(I)^{0.5}/(\epsilon_r T)^{0.5} \quad (8)$$

where I is the concentration of ions in water which can be related to the pH in the absence of salts such as NaCl, by $I = 10^{-pH}$ for pH $\leq$ 7 and $I = 10^{-(14-pH)}$ for pH > 7. Ψ is positive and increases with decreasing pH below the isoelectric point (point of zero charge where $\Psi = 0$) and is negative and decreases with increasing pH above the isoelectric point.[23−25] Experimentally measured Ψ of alumina for different pH has been used[25] for these computations. Since V_R depends on Ψ^2, on either side of the isoelectric point V_R is positive. At the isoelectric point, since $\Psi = 0$, there is no repulsive barrier and rapid aggregation takes place.[26] The isoelectric pH for alumina[23] is 9.1. W is given by[26]

$$W = 2r_p \int_0^\infty B(h) \exp\{(V_R + V_A)/k_B T\}/(h + 2r)^2 \, dh \quad (9)$$

where $B(h)$ is the factor that takes the hydrodynamic interaction into account. We have applied the widely used expression for $B(h)$[17,22,26] by Honing et al.[27]

$$B(h) = \frac{6(h/r_p)^2 + 13(h/a) + 2}{6(h/r_p)^2 + 4(h/a)} \quad (10)$$

Equation 9 shows that W is a strong function of r_p and decreases rapidly with decreasing r_p. Substituting W in the expression for t_p, it can be seen that t_p is a strong function of r_p; it decreases with decreasing r_p, and t_p is also a function of Ψ, pH, and Λ.

Figure 2 shows t_p for different radii of alumina nanoparticles and indicates that t_p decreases significantly with decreasing nanoparticle size. The reason for this behavior is because, at the same volume fraction, smaller particles are closer together than larger particles, which leads to a higher attraction due to van der Waals forces. Figure 2 also shows t_p for pH = 5.0 and pH = 9.1 (the isoelectric point for alumina). At pH = 9.1, t_p is very small because $\Psi = 0$ for alumina at this pH, making the repulsive energy zero. Figure 2 also shows that t_p decreases with increasing temperature because with increasing temperature BM increases, leading to a higher probability for particles to aggregate.

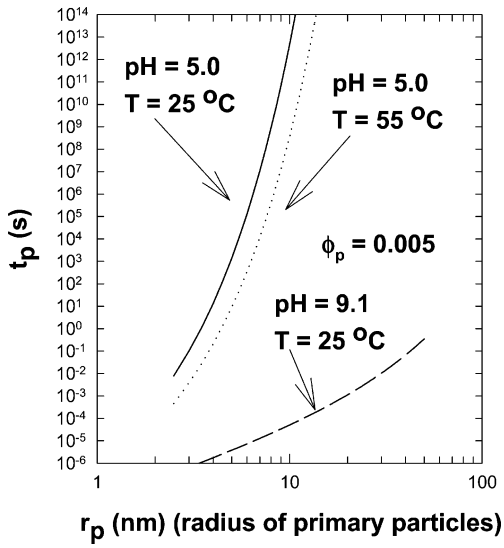

Figure 2. Dependence of aggregation time constant (t_p) on nanoparticle size, pH, and temperature. Note that the ζ potential for alumina at pH = 9.1 is zero (the isoelectric point). Therefore, t_p is very small at pH = 9.1.

In previous papers,[8,9] we showed the enhancement in k due to microconvection is related to a Brownian Reynolds number given by $Re = 2\upsilon r\rho_f/\mu$ where ρ_f is the density of the liquid and r is the radius of the particles. For an aggregate, the effective radius, r_{eq}, for the definition of Re is given by defining an equivalent sphere of the same volume as the volume of the nanoparticles in the aggregate. Therefore, it can be shown that $r_{eq}/r_p = (1 + t/t_p)^{0.333}$. For completely dispersed nanoparticles, $r = r_p$. The effective k due to convective enhancement is given by[8,9]

$$k/k_l = (1 + A \times Re^m Pr^{0.333}\phi) \quad (11)$$

where Pr is the Prandtl number, k_l the conductivity of the base liquid, and A and m are constants determined from experiments.[8,9] For metal oxide nanoparticles (Al_2O_3 and CuO), A was found to be 4×10^4 and $m = 2.5 \pm 15\%$. For an aggregate, Re is calculated using the Brownian speed, υ, of the aggregate based on the mass of the aggregate and r_{eq}.

For modeling the contribution due to conduction for the aggregated system, we have used the approach of Wang et al.[13] The conductivity of the aggregates is based on the Bruggeman model, as it takes into account the percolation effects due to direct contact between the particles. Therefore, the conductivity of an aggregate (k_a) is given by

$$(1 - \phi_{int})(k_l - k_a)/(k_l + 2k_a) + \phi_{int}(k_p - k_a)/(k_l + 2k_a) = 0 \quad (12)$$

where ϕ_{int} (the volume fraction of particles in the aggregate) is given by[28] $\phi_{int} = (R_a/r_p)^{d_f-3} = (1 + t/t_p)^{(d_f-3)/d_f}$ with the condition that the maximum value of $\phi_{int} = 1$ and the

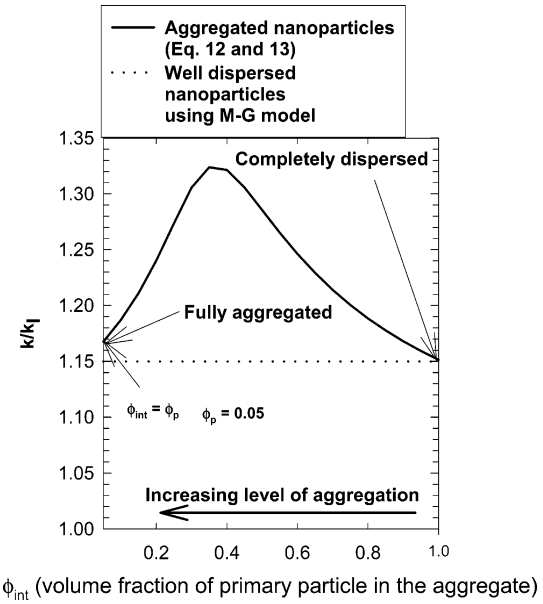

Figure 3. Effect of aggregation on the conductive contribution to *k*. Due to aggregation, percolation in the aggregates can lead to enhancement in *k*. This figure also shows that for a well-dispersed system the model reduces to the M−G model.[34]

minimum value of $\phi_{int} = \phi_p$, as discussed before. Once k_a is known from eq 12, the overall conductive contribution is given by the M−G model[34] where the volume fraction of the aggregates is used. Therefore, the overall conductive contribution is given by[34]

$$k/k_l = ([k_a + 2k_l] + 2\phi_a[k_a - k_l])/([k_a + 2k_l] - \phi_a[k_a - k_l]) \quad (13)$$

ϕ_a is calculated by the condition that $\phi_p = \phi_{int}\phi_a$. For the well-dispersed case, $\phi_{int} = 1$ and $\phi_a = \phi_p$, and eqs 12 and 13 show that *k* reduces to the M−G model for a well-dispersed system.

Results and Discussion. Figure 3 shows the conduction-based thermal conductivity for $\phi_p = 0.05$ as a function of ϕ_{int} based on eqs 12 and 13. Figure 3 also shows the thermal conductivity for a well-dispersed system by applying the M−G model (eq 12), and clearly indicates that enhancement due to conduction can increase due to aggregation as compared with a well-dispersed system, depending on the value of ϕ_{int} as discussed earlier. The limiting value in Figure 3 ($\phi_{int} = \phi_p$) is slightly higher than that from the M−G model because of the percolation effects in the agglomerate. Therefore, aggregation can enhance the conduction contribution only if the aggregates are well dispersed, not when one large aggregate is formed. For various conditions for $\phi_p = 0.05$ (different pH, *t*, *T*, r_p), we have found that the maximum in the conductive component (i.e., the enhancement due to aggregation) of *k* occurs at $\phi_{int} \approx 0.35$ and $\phi_a \approx \phi_p/0.35$. This means that *k* due to conduction increases for $\phi_p < \phi_{int} < 0.35$ and decreases for $0.35 < \phi_{int} < 1$. At $\phi_{int} = 1$, the nanoparticles are completely dispersed, and at $\phi_{int} = \phi_p$, they are completely aggregated.

The combined effects of convection and conduction using the method from our earlier papers,[8,9] where now the conduction contribution includes aggregation, are presented in Figure 4. The overall conductivity enhancement based on our earlier work[8,9] is given by: enhancement due to convection X enhancement due to conduction. *k* initially increases with decreasing r_p, reaches a peak, and then decreases due to aggregation effects. This behavior wrt particle size was also experimentally observed by Xie et al.[1] for alumina nanoparticles in ethylene glycol (EG). Figure 4 also shows the combined convective and conductive *k* for a well-dispersed system and demonstrates that the proposed model reduces to the well-dispersed behavior for no aggregation. For comparison, k/k_l for a well-dispersed system considering only conductive effects and ignoring convective effects is also calculated using the M−G model[8]. k/k_l based on a purely conductive model—without considering aggregation—is independent of the size of the nanoparticles.

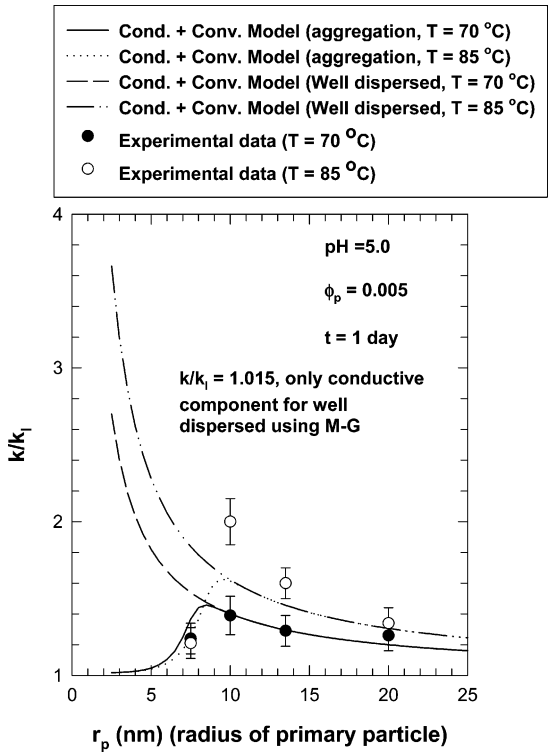

Figure 4. Thermal conductivity as a function of nanoparticle radius. Conduction-based M−G model for well-dispersed particles gives $k/k_l = 1.015$ for all particle sizes. Reduction in *k* after the peak takes place because of aggregation, leading to substantial reduction in the convective component.

We performed a controlled experimental investigation to observe the impact of decreasing particle size on *k*. Alumina nanoparticles were purchased from Nanotechnologies Inc. and suspended in the base fluid (water) using an ultrasonicator. The temperature oscillation technique and the corresponding experimental setup, described in detail in ref 29, were applied to measure the thermal conductivity of nanofluids. We performed separate experiments to measure the thermal conductivity of alumina−water nanofluids with particle radii of 7.5, 10, 13.5, and 20 nm, all of them with $\phi = 0.5\%$. Figure 4 shows the comparison between the experimental data and the aggregation model with $m = 2.125$. The pH of the solution was 5 to prevent rapid aggregation.

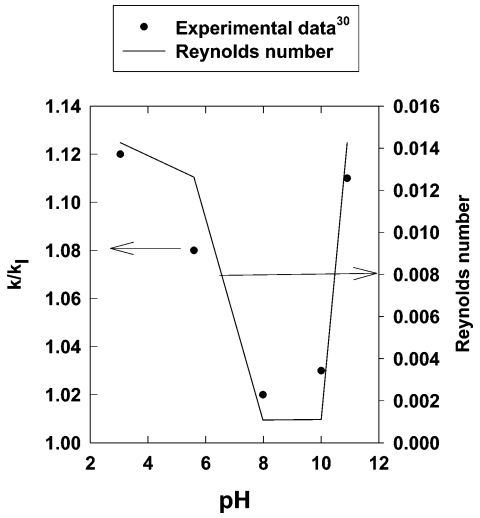

Figure 5. Effect of pH on thermal conductivity. Both the Brownian Reynolds number and thermal conductivity follow the same trend. At pH = 8 and 10, the ζ potential is very small leading to a significant reduction in the repulsive force which results in substantial aggregation.

The experimental data shown in Figure 4 were collected approximately 24 h from the time of preparation of the nanofluid samples. The data were taken at high temperatures to increase the effect of Brownian convection. Data for some of the other temperatures are not included for brevity. Figure 4 shows that the proposed model is in reasonable agreement with the experimental data, and both the experimental data and the model show a peak in k wrt to the size of the nanoparticles.

Another point to notice from Figure 4 is that the maxima in k shift to larger particle size with increasing temperature. This is because the increase in temperature leads to an increase in aggregation, since W decreases due to the increase in the thermal energy, making it easier for the particles to overcome the repulsive barrier leading to aggregation at larger particle sizes.

Lee et al.[30] recently measured k and Ψ for CuO/water-based NF for different pH at very low volume fraction ($\leq$ 0.3%). Lee et al.[30] reported that the nanoparticles were already aggregated before they were mixed in water. The size of the pristine aggregated nanoparticles was not known in their study. Therefore, we have compared their experimental data with the aggregation model only qualitatively. Due to the very small volume fraction, the conduction component is very small. Figure 5 shows the comparison between the measured k/k_l and the Brownian Reynolds number, $Re = 2\upsilon r_{eq}\rho_f/\mu$. Figure 5 indicates that both k/k_l and Re follow the same trend. Around pH = 8, Ψ is very small, leading to significant aggregation. To calculate t_p, we have used the W calculated by Lee et al.,[30] however at pH = 11 they underestimated W because of their data fitting. Thus, for pH = 11, we recalculated W.

Figures 6 and 7 show the effect of T on the k enhancement. Figure 6 shows that k/k_l increases with increasing temperature depending on r_p, which is in line with experimental data from two groups (Das et al.[1] and Chon et al.[3]), however Masuda et al.[1] reported a *decrease* in k/k_l wrt T. Likewise, Figure 7 shows that, for r_p = 16 nm, k/k_l *decreases* with increasing T. This is because at T = 25 °C, ϕ_{int} = 0.35 (k/k_l is maximum

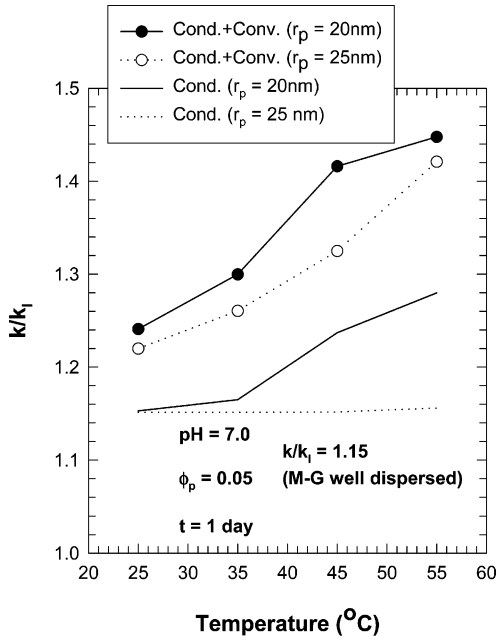

Figure 6. Effect of temperature on conductivity (k/k_l) for relatively large particles (r_p = 20, 25 nm). Results show that, depending on the size of the nanoparticles, the conductive contribution to k can also increase with temperature which is not possible for well-dispersed particles (k/k_l = 1.15 for well-dispersed particles according to the M−G model for all temperatures). The trend and the magnitude of the results are consistent with the data from Das et al.[3]

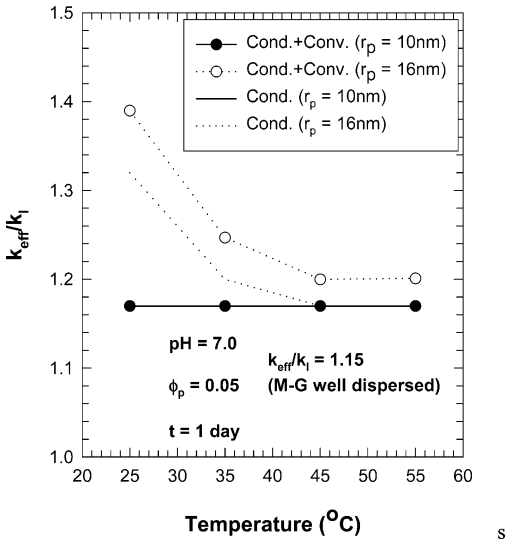

Figure 7. Effect of temperature on conductivity (k/k_l) for relatively small particles (r_p = 10, 16 nm). Results show that, depending on the size of the nanoparticles, the relative conductivity can decrease with temperature which is not possible for well-dispersed particles. The trend and the magnitude of the results are consistent with the data by Masuda et al.[2] Note that individually neither the conduction nor the convection model for well-dispersed particles will ever show any decrease in k/k_l with increasing temperature. The probability of aggregation increases with increasing temperature due to the reduction in the aggregation time constant t_p (Figure 2).

at this ϕ_{int} as mentioned earlier), at $T = 35$ °C, $\phi_{int} = 0.12$, and at $T = 45$ °C and 55 °C, $\phi_{int} = 0.05$. This shows that the system is completely aggregated at $T = 45$ and 55 °C, optimally aggregated for conduction at $T = 25$ °C, and more than optimally aggregated for $T = 35$ °C. For $r_p = 10$ nm, there is no change in k/k_l due to significant aggregation and no enhancement due to convection. Therefore, the conductive and conductive + convective curves overlay each other.

Wen and Ding[7] observed that k/k_l increased with T for CNT-based NF. For CNT, BM will be negligible. Typical conduction-based models without considering aggregation will give k/k_l independent of T, however Figure 6 shows that depending on the particle size the conductive effect (here for $r_p = 20$ nm) on k/k_l can also increase with temperature. This can again be explained based on the value of ϕ_{int} at different temperatures. Although the conductive model has been developed for spherical particles, the same physics can be applied for CNT-based NF.

Since V_R depends on Ψ^2, any error in Ψ can lead to significant error in the location of the maximum of the k enhancement, however the general trend will still remain the same. We recommend that any experimental work should always report (1) Ψ, (2) pH, (3) t after which the experiments were conducted, and (4) the size distribution of nanoparticles for fair comparison and modeling. Significant aggregation will also lead to significant sedimentation, which we have ignored here. Significant sedimentation will also affect the aggregation process. We have ignored the thermal boundary resistance (interface resistance), however it can be incorporated in calculating the thermal conductivity of the aggregate using the model by Every et al.[31] for a percolating system. The conductive contribution to k is not important for a very small volume fraction, which makes the impact of interface resistance negligible.

The aggregation considered in this paper is for a stationary system, which is also known as perikinetic aggregation.[32] Convective heat transfer coefficient of nanofluids have also shown unusual behavior.[33] Aggregation kinetics changes drastically in flowing situations, where it is called orthokinetic aggregation. Orthokinetic aggregation can change the convective performance of nanofluids and will be explored in future reports.

In experimental studies, it might also be possible that, due to colloidal forces, particle deposition can take place on the surface of the measuring device, which can lead to erroneous measurement and conclusions. Deposition kinetics can change the experimental conclusions. Particle deposition kinetics can also be modeled using established models from colloidal literature.[32]

In conclusion, we have combined aggregation kinetics based on colloidal chemistry with the physics of thermal transport to explain the thermal conductivity of nanofluids. Through this work, we have demonstrated that, apart from the physical properties such as thermal conductivity of the liquid, viscosity of the liquid, thermal conductivity of the nanoparticles, and density of the nanoparticles, the effective thermal conductivity of the colloidal nanosuspensions in a liquid depends on chemical parameters such as the Hamaker constant, the ζ potential, pH, and ion concentration. We have also shown that the conductive component of the thermal conductivity ratio can also increase with temperature depending on the chemistry of the solution. This behavior is not feasible without including the effects of chemistry and aggregation.

Acknowledgment. The authors gratefully acknowledge the support of the National Science Foundation, through a GOALI award (Award No. CTS-0353543) and the direct support provided by the Intel Corporation.

References

(1) Xie, H.; et al. *J. Appl. Phys.* **2002**, *91*, 4568.
(2) Masuda, H.; et al. *Netsu Bussei* **1993**, *4*, 227.
(3) Das, S. K.; et al. *Heat Transfer* **2003**, *125*, 567.
(4) Eastman, J. A.; et al. *Appl. Phys. Lett.* **2001**, *78*, 718.
(5) Wen, D.; Ding, Y. *Int. J. Heat Mass Transfer* **2004**, *47*, 5181.
(6) Hong, T.-K.; et al. *J. Appl. Phys.* **2005**, *97*, 064311.
(7) Patel, H. E.; et al. *Appl. Phys. Lett.* **2003**, *83*, 2931.
(8) Prasher, R. S.; et al. *Phys. Rev. Lett.* **2005**, *94*, 025901.
(9) Prasher, R. S.; et al. *J. Heat Transfer* **2006**, *128*, 588.
(10) Jang, S.; Choi, S. U. S. *Appl. Phys. Lett.* **2004**, *84*, 4316.
(11) Koo, J.; Kleinstreuer, C. *J. Nanopart. Res.* **2004**, *5*, 577.
(12) Chon, C. H.; et al. *Appl. Phys. Lett. 87*, 153107.
(13) Wang, B.-X.; et al. *Int. J. Heat Mass Transfer* **2003**, *46*, 2665.
(14) Keblinski, P.; et al. *Int. J. Heat Mass Transfer* **2002**, *45*, 855.
(15) Keblinski, P.; et al. *Mater. Today* **2005**, *36*, June.
(16) Russel, W. B.; et al. *Colloidal Dispersion*; Cambridge University Press: Cambridge, U.K.
(17) Hunter, R. J. *Foundations of Colloid Science*; Oxford University Press: New York, 2001.
(18) Bordi, F.; et al. *Physica A* **1990**, *164*, 663.
(19) Wen, D.; Ding, Y. *J. Thermophys. Heat Transfer* **2004**, *18*, 481.
(20) Hanus, L. H.; et al. *Langmuir* **2001**, *17*, 3136.
(21) Waite et al. *J. Colloid Interface Sci.* **2001**, *241*, 333.
(22) Hiemenz, P. C. *Principles of Colloid and Surface Chemistry*; Marcel Dekker: New York, 1997.
(23) Yopps, J. A.; Fuerstenau, D. W. *J. Colloid Interface Sci*. **1964**, *19*, 61.
(24) Wiese, G. R.; Healy, T. W. *J. Colloid Interface Sci.* **1975**, *51*, 427.
(25) Im, D. J.; et al. *J. Mater. Sci*. **1998**, *33*, 2931.
(26) Schudel, M.; et al. *J. Colloid Interface Sci.* **1997**, *196*, 241.
(27) Honing, E. P.; et al. *J. Colloid Interface Sci.* **1971**, *36*, 97.
(28) Potanin, A. A.; et al. *J. Chem. Phys*. **1995**, *102*, 5845.
(29) Bhattacharya, P.; et al. *Int. J. Heat Mass Transfer*, in press.
(30) Lee, D.; et al. *J. Phys. Chem. B* **2006**, *110*, 4323.
(31) Every, Y.; et al. *Acta Metall. Mater*. **1992**, *40*, 123.
(32) M. Elimelech et; al. *Particle Deposition and Aggregation, Measurement, Modeling and Simulation*; Butterworth-Heinemann: Woburn, MA, 1995.
(33) Buongiorno, J. *J. Heat Transfer* **2006**, *128*, 240.
(34) Nan, C.-W.; et al. *J. Appl. Phys*. **1997**, *81*, 6692.

NL060992S